DOI: 10.1002/asia.201100637

Selective, Cytotoxic Organoruthenium(II) Full-Sandwich Complexes: A Structural, Computational and In Vitro Biological Study

Bradley T. Loughrey,*[a] Benjamin V. Cunning,[b] Peter C. Healy,[a] Christopher L. Brown,[b] Peter G. Parsons,[c] and Michael L. Williams[a]

Abstract: A structurally diverse range of lipophilic, cationic η^6-arene η^5-cyclopentadienyl (η^5-Cp*) full-sandwich complexes of ruthenium(II) have been prepared and structurally characterized by Fourier-transform IR and NMR spectroscopy, electrospray mass spectrometry, and elemental microanalyses. Computational experiments incorporating the Hartree–Fock theory and the second-order Møller–Plesset perturbation theory predict each complex to possess a uniform δ+ electrostatic potential, with the cationic charge of the $[RuCp^*]^+$ moiety completely delocalizing throughout the molecular structure of each metallocene. In vitro cytotoxicity studies demonstrate these delocalized lipophilic cations to be potent growth inhibitors of eleven unique tumorigenic cell lines, while exhibiting significantly lower levels of toxicity towards both a normal human fibroblast and a mouse macrophage cell line. Single-crystal X-ray structural determinations are additionally reported for five complexes, $[Ru(\eta^6\text{-}C_6H_5(CH_2)_2CH_3)(\eta^5\text{-}C_5(CH_3)_5)]BPh_4$, $[Ru(\eta^6\text{-}C_6H_5CO_2CH_2CH_3)(\eta^5\text{-}C_5(CH_3)_5)]BF_4$, $[Ru(\eta^6\text{-}C_{10}H_8)(\eta^5\text{-}C_5(CH_3)_5)]BPh_4$, $[Ru(\eta^6\text{-}C_{14}H_{10})(\eta^5\text{-}C_5(CH_3)_5)]BPh_4$, and $[Ru(\eta^6\text{-}C_{16}H_{10})(\eta^5\text{-}C_5(CH_3)_5)]BPh_4$.

Keywords: arenes · cancer · cyclopentadienyl ligands · organometallic · ruthenium

Introduction

The significant involvement of metal ions and complexes in biological processes and systems has, over recent times, led to the realization that considerable opportunities exist for the design of metal-based therapeutics.[1] The landmark antitumor properties of cisplatin proved to be the herald of this new area of metallopharmaceutical research, with cisplatin and its numerous derivatives now firmly established as some of the most effective chemotherapeutic agents in clinical use.[2] Despite their overall success and clinical popularity, these platinum analogues suffer from disadvantages such as high secondary toxicity and both intrinsic and acquired drug resistance. Due to these limitations, it is of importance to discover metallopharmaceuticals that possess higher efficacy and activity while exerting fewer side-effects. In pursuit of this goal, a diverse array of complexes containing various transition metals have been evaluated, and elements such as cobalt, gallium, gold, iron, osmium, rhodium, and ruthenium have all produced promising libraries of novel anticancer complexes.[3] Out of the assortment of metallodrugs that contain metals other than platinum, ruthenium compounds have proven to be the most promising ones, with two coordination complexes, KP1019 and NAMI-A, having successfully completed phase I clinical trials.[4]

While the biological properties of inorganic coordination complexes have been thoroughly explored over the past decade, organometallic compounds have only been sparingly investigated, with recent results suggesting that these systems hold the potential to find use as therapeutic agents.[5] Essentially every class of metal–carbon bond has demonstrated some form of biological activity, including metal carbonyls, metal alkyls (found in naturally occurring systems such as the B_{12} series of vitamers), metal carbenes, organometallic compounds comprising metal–metal bonds, and metal–arene π-bond systems.[6] Ruthenium compounds comprising metal–arene bonds have seen particular success, with a plethora of interesting biological results having already been published for the Ru^{II} η^6-arene half-sandwich (pianostool) complexes.[5] The most prevalent examples of these molecules within the literature are the $[Ru(\eta^6\text{-arene})(Y{-}Z)L]^+$ (Y-Z = bidentate ligand, and L = monodentate anion) and RAPTA $[Ru(\eta^6\text{-arene})(Y\text{-}Z)PTA]$ (PTA = 1,3,5-triaza-7-phospha-adamantane) series of complexes, which display promising cytotoxic and antimetastatic activities, respectively.[7] Cationic organoruthenium full-sandwich complexes of the structure $[Ru(\eta^6\text{-arene})(\eta^5\text{-}C_5R_5)]^+$, in which R = H (Cp) or CH_3 (Cp*), have also been demonstrated to possess inter-

[a] Dr. B. T. Loughrey, Prof. P. C. Healy, Dr. M. L. Williams
Eskitis Institute for Cell and Molecular Therapies
Griffith University
Brisbane (Australia)
Tel: (+61) 07-373-57728
E-mail: bradley.loughrey@griffithuni.edu.au

[b] B. V. Cunning, Prof. C. L. Brown
Queensland Micro- and Nanotechnology Facility
Griffith University
Brisbane (Australia)

[c] Prof. P. G. Parsons
Drug Discovery Group
Queensland Institute of Medical Research
Brisbane (Australia)

esting in vitro biological activity.[8] The Cp derivatives, despite only exhibiting minimal cytotoxicity against human promyelocytic leukemia cell line HL-60, were found to interact with plasmid pBR322 DNA when investigated by atomic force microscopy, inducing significant supercoiling and kinking of the free DNA form. The Cp* derivatives, which are investigated in our research group, were found to exhibit potent cytotoxic activity in vitro, thereby inhibiting the growth of tumorigenic cell lines at concentrations comparable to that of cisplatin. The promising antitumor effects displayed by these cationic organoruthenium molecules prompted us to synthesize and biologically evaluate structurally diverse libraries of ruthenium(II)-based full-sandwich complexes (Figure 1; in which R represents a series of substituted functional groups including carboxylic acids, acid fluorides, esters, thioesters, ketones, alcohols, carbamates, amides, sulphonamides, and glycoconjugates.[9] The results of these studies demonstrated the cationic organoruthenium complexes to possess potent and selective antiproliferative activity towards a range of cancerous cell lines in vitro, including human skin carcinoma (MM96L) and two individual phenotypes of breast cancer (MCF7 and MDA-MB-231), with the degree of growth inhibition dependent on the size and lipophilicity of the arene ligand.[9] Of particular interest, however, was the relative inactivity of the neutral ruthenocenyl complexes when compared to their corresponding cationic derivatives. These mono-, 1,1′-di-, and pentasubstituted ruthenocenyl molecules were on average over two orders of magnitude less active than the respective cationic complexes, highlighting a relationship between positive charge and cytotoxic activity.[9] This structural dependence on both lipophilicity and a cationic charge, in addition to the notable specificity displayed by these complexes towards cancerous cells, thus suggests that these highly stable organoruthenium molecules may be exerting their cytotoxic effect in a manner similar to that of biologically active delocalized lipophilic cations (DLCs). As the name suggests, DLCs are lipophilic compounds that carry a positive charge delocalized across the surface of their molecular structure. DLCs have been shown through a number of studies to possess the capability to rapidly permeate cellular plasma and inner mitochondrial membranes.[10] Once inside the mitochondrial organelle, they concentrate within the lipid boundary in response to the negative mitochondrial membrane potential, ultimately triggering cell death through the mitochondrial pathway.[10]

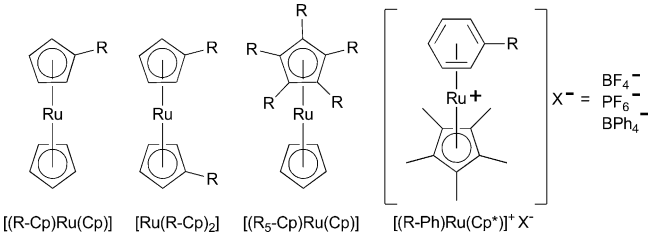

Figure 1. A focused library of organoruthenium full-sandwich complexes previously evaluated for antitumor activity; R represents substituted functional groups such as carboxylic acids, acid fluorides, esters, thioesters, ketones, alcohols, carbamates, amides, sulphonamides, and glycoconjugates.

In the present study, we endeavored to gain greater insight into the cytotoxic profile of these lipophilic organoruthenium cations through the in vitro evaluation of a structurally diverse series of molecules against a panel of thirteen different cell lines (including both tumorigenic and normal cells). Computational and structural experiments were also performed as a means of investigating how the cationic charge of the $[Ru^{II}Cp^*]^+$ moiety is distributed throughout the molecular structure of each metallocene.

Results and Discussion

Synthesis, Characterization, and Structural Analysis

Modern preparation of η^6-arene ruthenium η^5-pentamethylcyclopentadienyl complexes can be achieved through a plethora of multi-step synthetic routes, with the most popular methods often involving the preparation of labile, dimeric ruthenium starting materials (either $[Ru(\eta^6\text{-}C_6H_6)Cl_2]_2$ or $[Cp^*RuCl_2]_2$).[11] The former readily reacts with HCp* under ultraviolet radiation in the presence of acetonitrile as solvent to form $[(arene)Ru(Cp^*)]^+$ complexes, while the latter opens up a variety of additional synthetic mechanisms involving aromatic ligands and various reducing agents.[12] Reduction of $[Cp^*RuCl_2]_2$ with $LiBEt_3H$ yields a ruthenium(II) tetramer of the structure $[Cp^*Ru(\mu_3\text{-}Cl)]_4$, which undergoes facile halide abstraction when exposed to $AgCF_3SO_3$ in acetonitrile. This forms the solvated, labile half-sandwich complex $[Cp^*Ru(CH_3CN)_3]CF_3SO_3$, which can further react in the presence of aromatic ligands to produce $[Ru(arene)(Cp^*)]^+$ complexes in good yield. The highly arenophilic nature of $[Cp^*Ru(\mu_3\text{-}Cl)]_4$ can also be exploited in aqueous media under microwave irradiation, with exposure of the tetramer to aromatic ligands under these conditions, thus forming a diverse range of water soluble [(Cp*)Ru(arene)]Cl salts with no noticeable by-products. An alternate route involves the quantitative, two-step formation of alkoxoruthenium(II) complexes $[Cp^*Ru(O\text{-}alkyl)]_2$ through the reaction between $[Cp^*RuCl_2]_2$ and potassium carbonate in various alcohol solvents. These alkoxo intermediates, when in the presence of an aromatic ligand and suitable proton donor, will readily facilitate arene metalation. A similar procedure achieving comparable yields has also been undertaken using $NaOCH_3$ as a direct replacement to potassium carbonate. Preparative routes to η^6-arene ruthenium η^5-pentamethylcyclopentadienyl cations that did not involve the use of ruthenium dimer complexes were originally pioneered by Kudinov et al.,[13] with the initial method involving the reaction between ruthenium trichloride hydrate, aromatic ligands, and HCp* in refluxing ethanol.

The prior described methodologies each possess their own inherent advantages and disadvantages, with each procedure

ultimately capable of preparing various libraries of [Ru(arene)(Cp*)]$^+$ full-sandwich complexes in good to moderate yields. For the purposes of our investigations, it was of interest to incorporate a synthetic procedure that was facile, convenient, and eligible for use with a wide variety of aromatic starting materials. As these organoruthenium complexes were to undergo in vitro cytotoxic evaluation, it was also necessary to ensure that the chosen synthetic technique produced analytically pure samples of the desired product. To fulfill these requirements, we incorporated a modified version of the aforementioned synthetic scheme developed by Kudinov and co-workers. The devised method is a facile, one-pot procedure that affords the user the capability of preparing structurally diverse libraries of η^6-arene ruthenium η^5-pentamethylcyclopentadienyl cations by a combinatorial synthetic approach. This approach proceeds readily without the use of ultraviolet or microwave irradiation, and avoids the requirement of preparing highly reactive starting materials (such as [Cp*Ru(μ_3-Cl)]$_4$ and [Cp*Ru(CH$_3$CN)$_3$]) prior to use. Incorporation of this method (Scheme 1) afforded the preparation of a series of cationic organoruthenium full-sandwich complexes (**1**–**12**) as air stable, crystalline tetraphenylborate salts. The reaction is initiated through heating ruthenium(III) trichloride hydrate in ethanol under reflux conditions. The alcohol acts as a gentle reducing agent, and this facilitates conversion of the ruthenium(III) transition metal into its +2 oxidation state. The arene ligand (Ar) and HCp* are then introduced, thereby prompting formation of the organoruthenium sandwich complex over a period of 8–12 hours. Following aqueous workup, the complex is isolated as a solid, crystalline material through a metathesis reaction involving an aqueous solution of sodium tetraphenylborate of appropriate strength. Pure samples of each complex are obtained after alumina filtration and recrystallization from acetone. Complexes were characterized using ^{1}H and ^{13}C NMR spectroscopy, ESI-MS, FT-IR spectroscopy, and elemental microanalysis. Single-crystal X-ray structural determinations of complexes **4**, **5a**, and **10**–**12** were also performed.

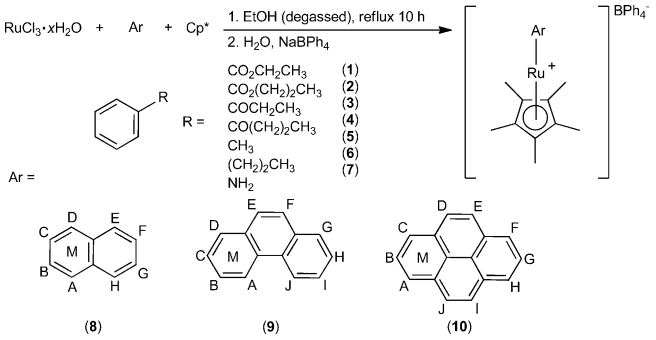

Scheme 1. Synthesis of ruthenium(II) arene Cp* full-sandwich complexes. Aromatic protons are labeled as per their ^{1}H NMR assignment; M designates the site of metal complexation.

The π complexation of the [Ru^{II}Cp*]$^+$ moiety to each aromatic ligand was confirmed post-synthesis by the characteristic upfield shift of the aromatic protons in the ^{1}H NMR spectra (Table 1). The obtained ^{13}C NMR data were in good agreement with the ^{1}H NMR results, thus presenting the expected shielding of the η^6-C$_6$H$_6$ carbons. The NMR data were also of use in determining the ruthenium metal coordination site for complexes incorporating polycyclic aromatic ligands (i.e., naphthalene (**10**), phenanthrene (**11**), and pyrene (**12**)). For each multi-ring system the metal undergoes π complexation to a terminal ring, thus shifting the ^{1}H NMR signals for this phenyl group upfield, while the NMR properties of the noncomplexed aromatic protons remain relatively unchanged. An X-ray crystallographic analysis of complexes (**10**–**12**) supports this result, with ORTEP representations (Figure 2) clearly demonstrating the ruthenium metal to favor π complexation to the terminal ring of each polycyclic ligand. These observations are in accordance with Clar's aromatic sextet theory, which predicts the terminal ring of polycyclic aromatic systems to possess the highest degree of aromaticity,[15] a property that is favorable for stable metal π-complexation.

Single-crystal X-ray structure determinations for complexes **4**, **5a**, and **10**–**12** demonstrate the ability of complexes to crystallize as discrete [Ru(η^6-arene)(η^5-Cp*)]$^+$ cations in the *Pbca* (**4**), $P2_1/c$ (**5a** and **12**) and $P2_1/n$ (**10** and **11**) space groups, respectively. Representative views of each structure are shown in Figure 2, while selected crystal data are available within Table 2. Geometric parameters and bond lengths for each structure (**4**, **5a**, and **10**–**12**) were found to be comparable with those previously published for complexes **1**, **2**, and **8**, respectively (Table 3).[8,14] For each compound the phenyl and Cp* rings are co-planar, with the angle formed by the ring centroids and ruthenium atom equaling 180.02° (**4**), 179.96° (**5a**), 176.44° (**10**), 177.77° (**11**), and 179.39° (**12**), respectively. The Cp*–arene interplanar separation is comparable for each complex, with an average distance of 3.52 Å. Ruthenium–carbon distances to both the η^5-Cp* and η^6-phenyl carbons (Table 2) are mostly comparable for each complex, with average values of 2.17 and 2.21 Å, respectively. Bond lengths between the metal and fusion arene carbons of complexes **10**–**12,** however, are observed to be significantly longer, with values ranging between 2.25 (**12**) and 2.30 Å (**10**). This increase in bond length indicates movement of the ruthenium atom away from the fusion carbons of the polycyclic ligands, a trend previously observed for [Ru(arene-R)(Cp*)]$^+$ complexes incorporating electron-withdrawing aromatic substituents.[9,16]

Computational Studies

Computational experiments using the Hartree–Fock (HF) theory and the second-order Møller–Plesset (MP2) perturbation theory were performed on each molecule as a means of further examining both the structural and electrostatic properties of complexes **1**–**12**.[17] Geometries of complexes **3**, **6**, **7**, and **9** were optimized at the HF level of theory with

Table 1. ^{1}H NMR chemical shift comparison between the prepared organoruthenium(II) full-sandwich complexes (**1**–**12**) and their noncomplexed aromatic ligands.[a]

Complex	Complexed arene	Noncomplexed arene	Upfield Shift
1	5.87 (s, 6H, C_6H_6)	7.27 (s, 6H, C_6H_6)	1.40
2	5.76-5.79 (m, 5H, C_6H_5)	7.08–7.13 (m, 3H, *meta, para*), 7.19–7.22 (m, 2H, *ortho*)	1.43 (*ortho*) 1.33 (*meta*) 1.33 (*para*)
3	5.83-5.85 (m, 5H, C_6H_5)	7.08–7.14 (m, 3H, *meta, para*), 7.20–7.23 (m, 2H, *ortho*)	1.38 (*ortho*) 1.27 (*meta*) 1.27 (*para*)
4	5.80-5.86 (m, 5H, C_6H_5)	7.08–7.13 (m, 3H, *meta, para*), 7.20–7.24 (m, 2H, *ortho*)	1.39 (*ortho*) 1.28 (*meta*) 1.28 (*para*)
5	6.07–6.09 (m, 3H, *meta, para*), 6.34–6.38 (m, 2H, *ortho*)	7.48–7.53 (m, 2H, *meta*), 7.61–7.66 (m, 1H, *para*), 7.94–7.97 (m, 2H, *ortho*)	1.60 (*ortho*) 1.43 (*meta*) 1.56 (*para*)
6	6.07–6.12 (m, 3H, *meta, para*), 6.36–6.38 (m, 2H, *ortho*)	7.49–7.52 (m, 2H, *meta*), 7.61–7.65 (m, 1H, *para*), 7.94–7.96 (m, 2H, *ortho*)	1.58 (*ortho*) 1.41 (*meta*) 1.53 (*para*)
7	6.08–6.10 (m, 3H, *meta, para*), 6.43–6.45 (m, 2H, *ortho*)	7.43–7.47 (m, 2H, *meta*), 7.53–7.58 (m, 1H, *para*), 7.89–7.92 (m, 2H, *ortho*)	1.47 (*ortho*) 1.36 (*meta*) 1.47 (*para*)
8	6.05–6.09 (m, 3H, *meta, para*), 6.42–6.44 (m, 2H, *ortho*)	7.43–7.47 (m, 2H, *meta*), 7.53–7.58 (m, 1H, *para*), 7.89–7.92 (m, 2H, *ortho*)	1.48 (*ortho*) 1.38 (*meta*) 1.49 (*para*)
9	5.20 (d, 2H, C_6H_5 *ortho*), 5.42-5.44 (m, 1H, C_6H_5 *para*), 5.56-5.59 (m, 2H, C_6H_5 *meta*)	6.44-6.49 (m, 1H, C_6H_5 *para*), 6.52-6.56 (m, 2H, C_6H_5 *ortho*), 6.96-7.01 (m, 2H, C_6H_5 *meta*)	1.34 (*ortho*) 1.41 (*meta*) 1.04 (*para*)
10	6.11-6.13 (m, 2H, aromatic (B, C)), 6.67-6.69 (m, 2H, aromatic (A, D)), 7.60-7.64 (m, 2H, aromatic (F, G)), 7.66-7.70 (m, 2H, aromatic (E, H))	7.49-7.52 (m, 4H, aromatic (B, C, F, G)), 7.89-7.92 (m, 4H, aromatic (A, D, E, H))	1.23 (A) 0.23 (E) 1.39 (B) -0.11 (F) 1.39 (C) -0.11 (G) 1.23 (D) 0.23 (H)
11	6.19-6.24 (m, 2H, aromatic (B, C)), 6.62-6.64 (m, 1H, aromatic (D)), 7.39-7.42 (m, 2H, aromatic (H, I)), 7.78-7.80 (m, 2H, aromatic (A, E)), 7.98-8.03 (m, 2H, aromatic (F, G)), 8.57-8.59 (m, 1H, aromatic (J))	7.62-7.71 (m, 4H, aromatic (B, C, H, I)), 7.83 (s, 2H, aromatic (E, F)), 7.98 (d, 2H, aromatic (D, G)), 8.81 (d, 2H, aromatic (A, J))	1.02 (A) -0.18 (F) 1.45 (B) -0.03 (G) 1.45 (C) 0.26 (H) 1.35 (D) 0.26 (I) 0.04 (E) 0.23 (J)
12	6.36-6.39 (m, 1H, aromatic (B)), 6.75-6.77 (m, 2H, aromatic (A, C)), 7.72-7.74 (m, 2H, aromatic (D, J)), 8.08-8.12 (m, 1H, aromatic (G)), 8.26-8.29 (m, 4H, aromatic (E, F, H, I))	8.04-8.08 (t, 2H, aromatic (B, G)), 8.17 (s, 4H, aromatic (D, E, I, J)), 8.28 (d, 4H, aromatic (A, C, F, H))	1.52 (A) 0.00 (F) 1.68 (B) -0.04 (G) 1.52 (C) 0.00 (H) 0.44 (D) -0.11 (I) -0.11 (E) 0.44 (J)

[a] δ_H in ppm. Coupling patterns, multiplicities, and assignments are shown in parentheses. All experiments were referenced against a deuterated DMSO internal standard (reference peak: $[D_6]$DMSO, ^{1}H $\delta = 2.49$ ppm).

the LanL2DZ basis set, with diagrammatic representations and selected bond parameters available as Figure 3 and Table 4, respectively.[18] Optimized geometries of **3**, **6**, **7**, and **9** are isostructural with those obtained through X-ray crystallographic analysis of complexes **1**, **2**, **4**, **5a**, **8**, and **10**—**12,** respectively (Table 3), with the only noticeable difference observed to be the Cp*–arene interplanar distances. The average computational interplanar separation for complexes **3**, **6**, **7**, and **9** is 3.87 Å, with ruthenium–carbon distances to both the η^5-Cp* and η^6-phenyl carbons (Table 4) possessing average values of 2.25 and 2.43 Å, distances significantly longer than the experimental averages discussed previously (3.52, 2.17, and 2.21 Å, respectively).

Electrostatic potential surfaces for complexes **2**–**12** were calculated and mapped on electron density surfaces by using structural parameters obtained through both computational structure optimization and X-ray structural analyses of each metallocene. The cc-pVDZ basis set was used for all atoms, with ruthenium parameters adjusted for the inclusion of a pseudo potential.[19] Predicted atomic charges for each complex were generated using Mulliken population analyses, with the electrostatic potential surfaces represented in Figure 4. The calculated electrostatic potential maps predict that the net positive charge of the $[RuCp^*]^+$ moiety is completely delocalized throughout the molecular structure of each metallocene, such that the complexes possess a uniform (slightly positive δ+) electrostatic potential. As expected, these calculations therefore suggest that $[(arene)Ru(Cp^*)]^+$ complexes exist as delocalized lipophilic cations, a property which would impact their behavior within biological systems.[10]

In Vitro Cytotoxic Evaluation

After verifying their purity, complexes **1**–**12** were subjected to cytotoxic evaluation using a sulforhodamine B (SRB) col-

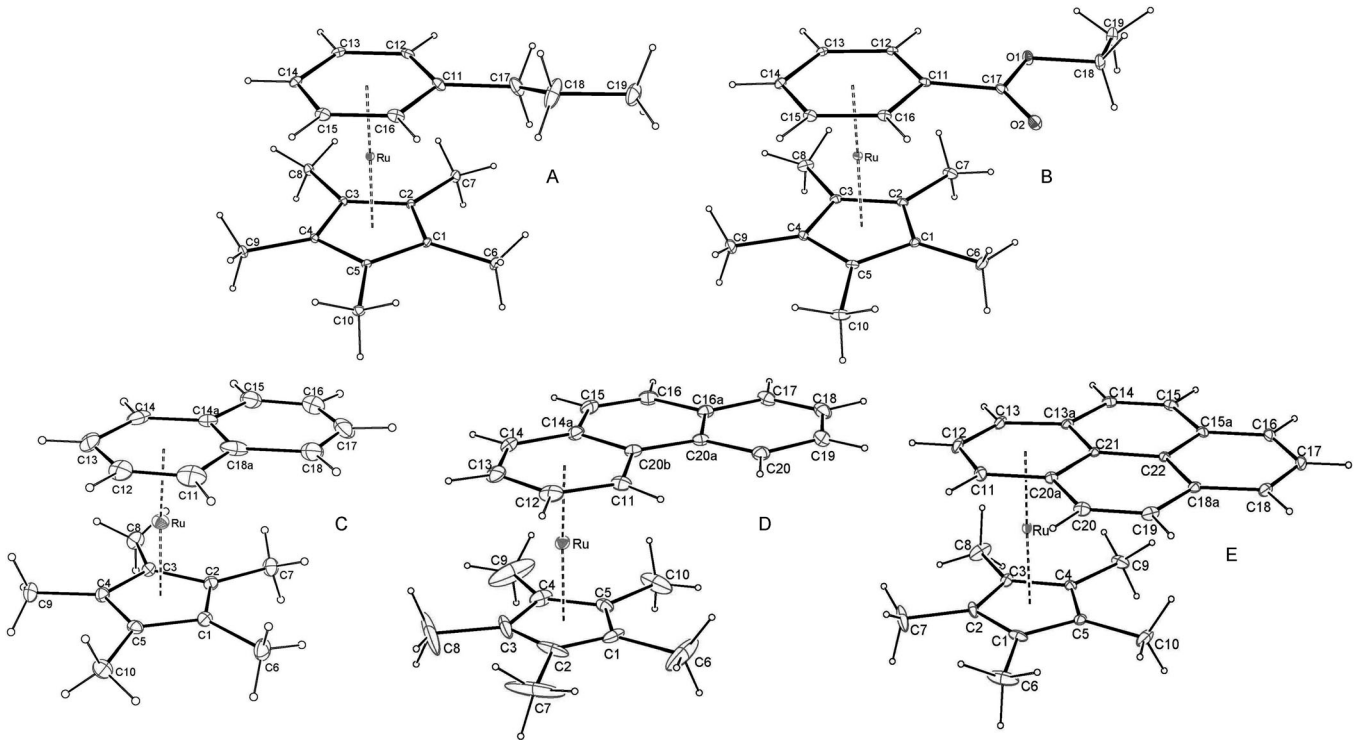

Figure 2. X-ray crystal structures with atom numbering schemes for (A) $[Ru(\eta^6\text{-}C_6H_5(CH_2)_2CH_3)(\eta^5\text{-}C_5(CH_3)_5)]BPh_4$ (**4**), (B) $[Ru(\eta^6\text{-}C_6H_5CO_2CH_2CH_3)(\eta^5\text{-}C_5(CH_3)_5)]BF_4$ (**5a**), (C) $[Ru(\eta^6\text{-}C_{10}H_8)(\eta^5\text{-}C_5(CH_3)_5)]BPh_4$ (**10**), (D) $[Ru(\eta^6\text{-}C_{14}H_{10})(\eta^5\text{-}C_5(CH_3)_5)]BPh_4$ (**11**), and (E) $[Ru(\eta^6\text{-}C_{16}H_{10})(\eta^5\text{-}C_5(CH_3)_5)]BPh_4$ (**12**). Thermal ellipsoids are drawn at 25% probability; counterions are omitted for clarity.

Table 2. Crystal data for $[Ru(\eta^6\text{-arene})(\eta^5\text{-Cp*})]^+$ complexes (**4**, **5a**, **10**–**12**).

Complex	**4**	**5a**	**10**	**11**	**12**
Formula	$C_{43}H_{47}BRu$	$C_{19}H_{25}O_2BF_4Ru$	$C_{44}H_{43}BRu$	$C_{48}H_{45}BRu$	$C_{50}H_{45}BRu$
Mol. Weight	675.7	473.3	683.7	733.7	757.7
Crystal System	Orthorhombic	Monoclinic	Monoclinic	Monoclinic	Monoclinic
Space Group	*Pbca*	$P2_1/c$	$P2_1/n$	$P2_1/n$	$P2_1/c$
a [Å]	18.506(3)	15.9234(2)	10.2731(2)	31.402(9)	10.5574(5)
b [Å]	16.730(2)	16.5056(2)	31.0155(9)	10.681(2)	14.8108(7)
c [Å]	22.325(3)	15.2162(2)	11.0446(3)	11.216(3)	24.2992(10)
α [°]	90	90	90	90	90
β [°]	90	92.180(1)	93.812(2)	97.560(2)	90.438(3)
γ [°]	90	90	90	90	90
V [Å^3]	6911.6(2)	3996.31(9)	3511.3(2)	3729.2(16)	3799.4(3)
Z	8	8	4	4	4
d_{calcd} [g cm^{-3}]	1.30	1.57	1.29	1.31	1.33
μ [mm^{-1}]	0.48	0.83	0.48	0.45	0.45
Crystal Size [mm]	0.65×0.58×0.54	0.45×0.40×0.36	0.28×0.18×0.09	0.40×0.20×0.15	0.34×0.21×0.18
$T_{min,max}$	0.74, 0.78	0.71, 0.75	0.88, 0.96	0.84, 0.94	0.86, 0.92
$2\theta_{max}$ [°]	55.0	55.0	50.0	50.0	50.0
N (total)	68 312	21 387	15 564	7217	13913
N (unique)	7927	9159	5903	6566	6401
N_o ($I>2\sigma(I)$)	6424	7920	4520	3377	5198
R_{int}	0.025	0.016	0.038	0.051	0.019
R_1	0.028	0.030	0.058	0.058	0.031
wRF^2 (all data)	0.072	0.080	0.140	0.185	0.084

orimetric assay for cell density determination following drug treatment in microtiter wells for 6 days.[20] A diverse panel of both tumorigenic and normal cell lines were chosen for this study: A549 (lung cancer), B16 (murine melanoma), CI80-13S (ovarian cancer), DU145 (prostate cancer grade II), HT29 (colon cancer), MCF7 (hormone-dependent breast cancer), MDA-MB-231 (hormone-independent breast cancer), MM418c5 (human melanoma), MM96L (human

CHEMISTRY
AN ASIAN JOURNAL

Table 3. Selected geometric parameters (Å) for organoruthenium(II) full-sandwich complexes, with atoms numbered as per Figure 2.

Complex	**1**[a]	**2**[a]	**4**	**5** (1)[b]	**5** (2)[b]	**8**[a]	**10**	**11**	**12**
Ru–C1	2.170(8)	2.147(8)	2.192(2)	2.183(2)	2.195(3)	2.192(2)	2.168(4)	2.128(7)	2.172(3)
Ru–C2	2.170(8)	2.178(7)	2.182(2)	2.179(2)	2.177(2)	2.175(2)	2.180(4)	2.112(12)	2.153(3)
Ru–C3	2.183(5)	2.167(7)	2.170(2)	2.179(2)	2.177(3)	2.175(2)	2.194(4)	2.134(11)	2.162(2)
Ru–C4	2.170(6)	2.149(8)	2.183(2)	2.178(3)	2.180(3)	2.164(2)	2.166(4)	2.151(9)	2.173(2)
Ru–C5	2.183(5)	2.167(7)	2.175(2)	2.191(3)	2.188(3)	2.173(2)	2.177(4)	2.156(7)	2.186(2)
Ru–C11	2.208(6)	2.208(8)	2.223(2)	2.205(2)	2.210(2)	2.191(2)	2.242(8)	2.221(7)	2.229(3)
Ru–C12	2.186(8)	2.215(8)	2.199(2)	2.214(2)	2.219(2)	2.210(3)	2.201(7)	2.190(9)	2.229(3)
Ru–C13	2.181(8)	2.219(8)	2.204(2)	2.221(2)	2.224(3)	2.217(3)	2.200(6)	2.197(9)	2.226(3)
Ru–C13a									2.263(3)
Ru–C14	2.208(6)	2.210(8)	2.209(2)	2.218(2)	2.220(3)	2.206(3)	2.190(6)	2.196(8)	
Ru–C14a							2.252(4)	2.254(7)	
Ru–C15	2.186(6)	2.213(8)	2.209(2)	2.226(3)	2.222(3)	2.206(3)			
Ru–C16	2.181(8)	2.182(7)	2.207(2)	2.216(3)	2.213(2)	2.184(3)			
Ru–C18a							2.303(6)		
Ru–C20a									2.250(2)
Ru–C20b								2.293(6)	
Ru–C21									2.249(2)
C11–C17		1.487(14)	1.518(4)	1.501(3)	1.504(3)	1.507(4)			
C17–O1				1.323(3)	1.321(4)				
C17–O2				1.203(3)	1.193(3)	1.204(3)			

[a] Structural parameters obtained from Gemel et al. (**1**), Navarro Clemente et al. (**2**) and Loughrey et al. (**8**), respectively.[8,14] [b] Structure of **5a** with two molecules in the asymmetric unit. X-ray data obtained using the BF_4^- counterion as crystals produced using the BPh_4^- counterion (**5**) provided data unsuitable for publication.

melanoma), PC3 (prostate cancer grade IV), T47-D (hormone-dependent breast cancer), RAW264 (a murine macrophage cell line), and NFF (neonatal foreskin fibroblasts). Each of these cell lines is susceptible to a variety of applied chemotherapeutics and also displays differing mechanisms of cross-resistance to drug treatment.

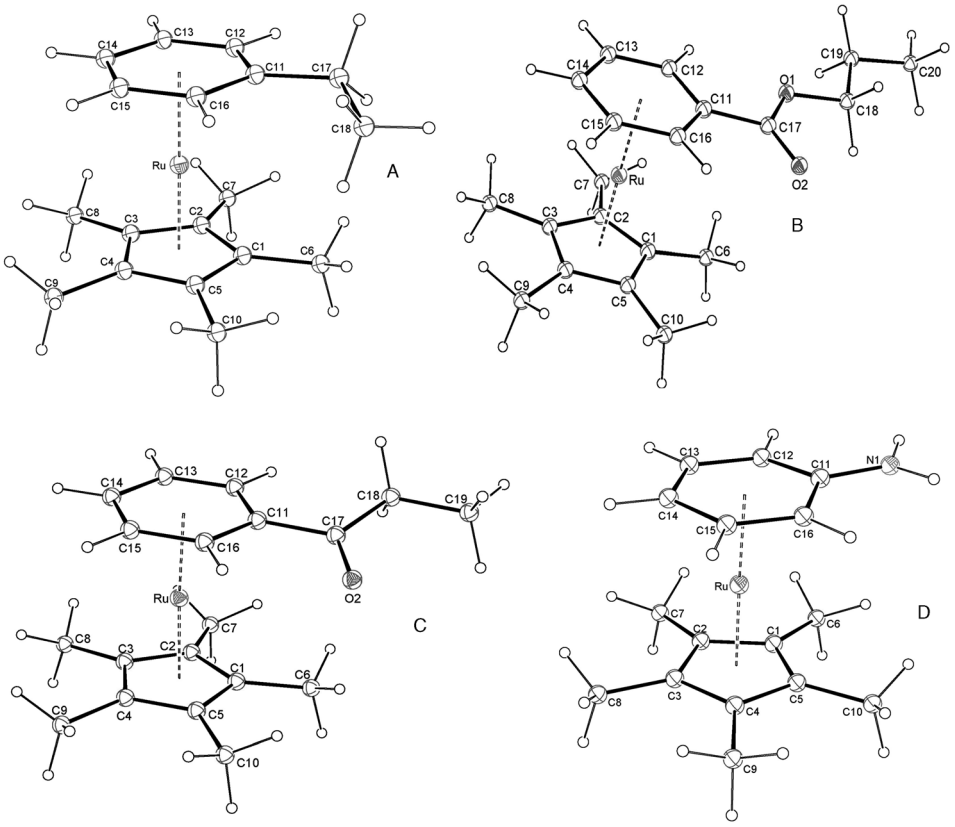

Figure 3. Computationally optimized structures with atom numbering schemes for (A) $[Ru(\eta^6\text{-}C_6H_5CH_2CH_3)(\eta^5\text{-}C_5(CH_3)_5)]^+$ (**3**), (B) $[Ru(\eta^6\text{-}C_6H_5CO_2(CH_2)_2CH_3)(\eta^5\text{-}C_5(CH_3)_5)]^+$ (**6**), (C) $[Ru(\eta^6\text{-}C_6H_5COCH_2CH_3)(\eta^5\text{-}C_5(CH_3)_5)]^+$ (**7**), and (D) $[Ru(\eta^6\text{-}C_6H_5NH_2)(\eta^5\text{-}C_5(CH_3)_5)]^+$ (**9**).

Results of this assay are listed (Table 5) and demonstrate these complexes to be cytotoxic and relatively selective growth inhibitors of all eleven tumorigenic cell lines, achieving IC_{50} values (concentration at which 50% of cell growth is inhibited) in the low micromolar range (0.03–37.6 μM). The average antiproliferative effect of these cationic organoruthenium complexes follows the sequence **12** > **11** > **10** > **4** > **6** ≈ **8** ≈ **3** > **2** > **1** > **5** > **7** > **9**, with cytotoxic activity again found to be dependent upon both the size and lipophilicity of the complexed η^6-arene ligand. Complexes **10**–**12**, which incorporate the large, hydrophobic polycyclic aromatic ligands naphthalene (**10**), phenanthrene (**11**), and pyrene (**12**) achieve the highest levels of growth inhibition recorded for complexes of this type, thereby registering IC_{50} values in the nanomolar range (0.03–0.35 μM).

Table 4. Selected calculated bond lengths (Å) for $[Ru(\eta^6\text{-}C_6H_5CH_2CH_3)(\eta^5\text{-}C_5(CH_3)_5)]^+$ (**3**), $[Ru(\eta^6\text{-}C_6H_5CO_2(CH_2)_2CH_3)(\eta^5\text{-}C_5(CH_3)_5)]^+$ (**6**), $[Ru(\eta^6\text{-}C_6H_5COCH_2CH_3)(\eta^5\text{-}C_5(CH_3)_5)]^+$ (**7**), and $[Ru(\eta^6\text{-}C_6H_5NH_2)(\eta^5\text{-}C_5(CH_3)_5)]^+$ (**9**).

Complex	3	6	7	9
Ru–C1	2.260	2.251	2.253	2.256
Ru–C2	2.257	2.252	2.254	2.256
Ru–C3	2.255	2.252	2.252	2.253
Ru–C4	2.254	2.252	2.251	2.260
Ru–C5	2.256	2.249	2.249	2.253
Ru–C11	2.460	2.398	2.412	2.521
Ru–C12	2.415	2.429	2.429	2.431
Ru–C13	2.411	2.435	2.433	2.406
Ru–C14	2.415	2.433	2.433	2.405
Ru–C15	2.410	2.427	2.424	2.406
Ru–C16	2.421	2.413	2.409	2.431
C11–C17	1.520	1.495	1.513	
C11–N1				1.366
C17–O1		1.331		
C17–O2		1.217	1.221	

Four human cancer cell lines were found to be particularly susceptible to growth inhibition under in vitro conditions, these being the rapidly dividing human melanoma cell line (MM96L), both hormone-dependent phenotypes of breast cancer (T47-D and MCF7), and the cisplatin-resistant ovarian cancer cell line (CI80-13S). Complexes **1**–**12** inhibit the growth of these cell lines at potencies 18.5-, 15.8-, 11.1-, and 10.9-fold greater than that displayed towards the control human fibroblast cell line (NFF). The cell lines A549, MDA-MB-231, HT29, PC3, and DU145 (which each exhibit a slow in vitro proliferation rate) were found to be more tolerant, however, with the complexes inhibiting these particular cell lines at potencies 2.9-, 4.9-, 5.8-, 6.0-, and 7.0-fold greater than that exhibited towards NFF.

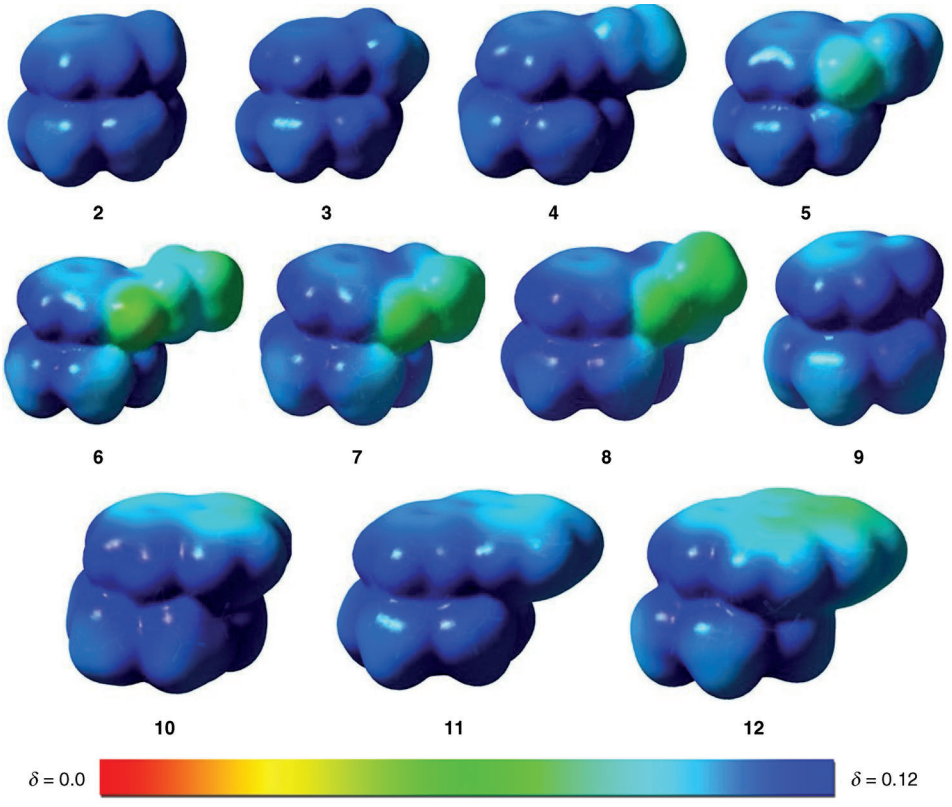

Figure 4. Electrostatic potential surfaces of organoruthenium(II) full-sandwich complexes **2**–**12**. The electrostatic potential is represented with a color scale ranging from red (0.00 au) to blue (+ 0.12 au).

Conclusions

A structurally diverse series of organoruthenium(II) full-sandwich complexes have been prepared in good yield and purity through a simple one-pot reaction of $RuCl_3{\cdot}xH_2O$, HCp*, and aromatic ligands in refluxing alcohol. Computational experiments incorporating the Hartree–Fock method and the second-order Møller–Plesset perturbation theory predict each complex to possess a uniform δ+ electrostatic potential, with the cationic charge of the $[RuCp^*]^+$ moiety completely delocalizing throughout the molecular structure of each metallocene. Cytotoxic evaluation of these delocalized lipophilic cations show them to be potent antitumor agents against a wide range of cancerous cell lines, while displaying significantly lower toxicity towards both the normal human fibroblast and mouse macrophage controls. Complexes are found to favor inhibition of rapidly dividing cancer cells including human melanoma (MM96L), two hormone-dependent phenotypes of breast cancer (T47-D and MCF7), and the cisplatin-resistant ovarian cancer cell line (CI80-13S). Cytotoxic activity is found to increase with size and lipophilicity of the attached aromatic ligand, with complexes incorporating the polycyclic aromatic groups naphthalene, phenanthrene, and pyrene registering IC_{50} values in the nanomolar range.

Experimental Section

General Procedures

All reactions were conducted under argon using standard Schlenk techniques unless stated otherwise. $[Ru(\eta^6\text{-}C_6H_5R)(Cp^*)]^+$ (where $R = CH_3$ (**2**), $CO_2(CH_2)_2CH_3$ (**6**), $CO(CH_2)_2CH_3$ (**8**), and NH_2 (**9**)) compounds were prepared and isolated using literature methods.[9] The identification and purity of these compounds was assured through comparison of experimentally attained characterization data with prior published literature values. Starting materials and solvents were obtained from a commercial supplier (Aldrich) and used as received. Fourier transform infrared spectroscopy (FT-IR) was

CHEMISTRY
AN ASIAN JOURNAL

Table 5. Inhibitory concentration that limits proliferation by 50% (IC_{50}) for the organoruthenium(II) full-sandwich complexes 1–12 against a range of cancer cell lines and two non-tumorigenic cell lines (RAW264 and NFF). Cisplatin (Csp) was incorporated for the purposes of a positive control.

Complex IC_{50} values [μM][a]	1	2	3	4	5	6	7	8	9	10	11	12	Csp
A549	12.2	12.7	8.14	7.05	24.1	10.1	32.2	9.72	36.1	1.31	1.31	0.36	
B16	11.8	12.5	8.25	3.63	18.5	8.04	14.1	8.58	36.5	1.24	1.24	0.94	
CI80-13S	4.05	3.86	3.21	2.88	3.78	2.72	13.0	2.92	4.45	0.44	0.44	0.10	3.20
DU145	7.86	8.17	6.73	3.96	7.75	4.98	8.38	4.27	12.2	0.54	0.54	0.11	1.78
HT29	8.32	9.84	6.86	3.83	7.40	4.25	8.23	3.95	37.6	0.41	0.41	0.48	
MCF7	6.71	4.99	2.89	2.24	5.57	2.33	4.31	3.00	4.73	0.34	0.34	0.25	1.80
MDA-MB-231	11.6	5.20	5.65	5.74	19.7	3.36	24.7	9.14	12.0	1.42	1.42	0.80	
MM418c5	5.98	6.32	4.51	2.44	7.96	3.77	12.2	5.21	10.3	0.36	0.36	0.17	0.80
MM96L	6.03	2.28	1.70	1.26	2.73	2.54	4.17	2.85	3.50	0.16	0.16	0.04	1.70
PC3	7.66	8.80	5.82	3.41	11.5	8.14	7.68	3.93	13.5	0.89	0.89	0.24	
T47-D	6.32	5.17	1.81	1.12	3.93	2.86	4.18	1.83	9.10	0.15	0.15	0.03	
RAW264	20.7	16.6	12.4	6.76	31.2	9.42	27.2	30.2	26.8	2.70	2.70	1.83	
NFF	37.9	92.2	30.7	18.1	48.5	10.6	101	32.7	98.2	2.38	2.38	1.02	3.30

[a] Errors are within the range of ±5–10% of the reported value. Results are the average of three separate experiments.

conducted on a Thermo Nicolet Nexus FT-IR spectrometer with all samples prepared as KBr discs. The following abbreviations apply to the intensity of peaks found within the spectra: vs = very strong; s = strong; m = medium; and w = weak. Electrospray ionization mass spectrometry experiments were conducted on a Waters ZQ 4000 mass spectrometer by direct injection. All data were processed using the Mass Lynx Version IV (IBM) software. ^{1}H and ^{13}C NMR spectra were obtained on a 400 MHz Varian Gemini NMR spectrometer with each sample being prepared in a solution of [D$_6$]DMSO. Peaks obtained for the deuterated solvent were used as internal reference points for the spectra (reference peaks: [D$_6$]DMSO, ^{1}H, $\delta = 2.45$ ppm, ^{13}C, $\delta = 39.5$ ppm). All signals were recorded using their appropriate chemical shift (δ in ppm), multiplicity, integral ratio, and coupling constants (Hz). The following abbreviations apply to the signal multiplicity of peaks within the spectra: s = singlet, d = doublet, t = triplet, and m = multiplet. Signals for the aromatic protons of complexes **10–12** were assigned according to the labeling system shown in Scheme 1. All deuterated solvents were supplied by Cambridge Isotope Laboratories and were used without further purification. Microanalyses were performed at the Microanalytical Unit of the University of Queensland.

*Synthetic Procedure for the Preparation of Complexes **1**, **3–5**, **5a**, **7**, and **10–12***

Ruthenium trichloride hydrate (0.20 g, 0.76 mmol) was transferred into the reaction vessel using ethanol (20 mL). This mixture was refluxed until all starting material had dissolved. Pentamethylcyclopentadiene (0.24 mL, 1.52 mmol) and the arene ligand (1.52 mmol) were added to the reaction mixture, and the resulting solution heated at reflux for a further 10 h. The solvent was concentrated in vacuo and the remaining residue dissolved in a water/diethyl ether partition mixture (20 mL/20 mL). The aqueous portion was retained and washed with diethyl ether (20 mL x3). The aqueous layer was then mixed slowly with 5 mL of a 0.30 M aqueous solution of sodium tetraphenylborate (**1, 3–5, 7, 10–12**) or ammonium tetrafluoroborate (**5a**), respectively. The resulting precipitate was filtered off and dried in vacuo. Complex **5a**, which incorporated the BF_4^- counter ion, required no further purification. The remaining tetraphenylborate complexes were redissolved in a minimum quantity of acetone and filtered through a short alumina column (neutral, 150 mesh) using acetone as the eluent. Analytically pure samples of the complexes were obtained after concentration of the acetone solvent in vacuo.

*[Ru(η^6-C$_6$H$_6$)(η^5-C$_5$(CH$_3$)$_5$)]BPh$_4$ (**1**)*

White powder, yield = 0.395 g, 82%; IR: $\tilde{\nu} = 3060$ (C–H aromatic, w, br), 2968 (C–H aliphatic, w, br), 2922 cm^{-1} (C–H aliphatic, w, br); NMR: ^{1}H ([D$_6$]DMSO): $\delta = 1.94$ (s, 15H, C$_5$(C$_5$H$_{15}$)), 5.87 (s, 6H, C$_6$H$_6$), 6.76–6.80 (m, 4H, B(C$_6$H$_5$)$_4$ *para*), 6.90–6.93 (m, 8H, B(C$_6$H$_5$)$_4$ *meta*), 7.15–7.20 ppm (m, 8H, B(C$_6$H$_5$)$_4$ *ortho*); ^{13}C ([D$_6$]DMSO): $\delta = 10.3$ (C$_5$-(*C*$_5$H$_{15}$)), 87.1 (C$_6$H$_6$), 95.9 (*C*$_5$(C$_5$H$_{15}$), 121.5 (4CH, B(C$_6$H$_5$)$_4$), 125.3 (8CH, B(C$_6$H$_5$)$_4$), 135.5 (8CH, B(C$_6$H$_5$)$_4$), 162.4, 163.0, 163.7, 164.3 ppm (4CH, B(C$_6$H$_5$)$_4$, signals split by ^{11}B); ESMS (*m*/*z*): positive ion, calcd *m*/*z* for [(η^5-C$_5$(CH$_3$)$_5$)Ru(η^6-C$_6$H$_6$)$^+$]: 314.44, found: 315 (100%), negative ion, calcd *m*/*z* for B(C$_6$H$_5$)$_4^-$: 319.25, found: 319 (100%); elemental analysis, calcd (%) for C$_{40}$H$_{41}$BRu: C 75.8, H 6.53; found: C 75.9, H 6.69.

*[Ru(η^6-C$_6$H$_5$CH$_2$CH$_3$)(η^5-C$_5$(CH$_3$)$_5$)]BPh$_4$ (**3**)*

White powder, yield = 0.403 g, 77%; IR: $\tilde{\nu} = 3052$ (C–H aromatic, m, br), 2974 (C–H aliphatic, m, br), 2922 cm^{-1} (C–H aliphatic, w, br); NMR: ^{1}H ([D$_6$]DMSO): $\delta = 1.15$ (t, 3H, CH$_2$*CH*$_3$), 1.89 (s, 15H, C$_5$(C$_5$H$_{15}$)), 2.33 (q, 2H, *CH*$_2$CH$_3$), 5.83–5.85 (m, 5H, C$_6$H$_5$), 6.76–6.81 (m, 4H, B(C$_6$H$_5$)$_4$ *para*), 6.89–6.94 (m, 8H, B(C$_6$H$_5$)$_4$ *meta*), 7.15–7.20 ppm (m, 8H, B-(C$_6$H$_5$)$_4$ *ortho*); ^{13}C ([D$_6$]DMSO): $\delta = 10.0$ (C$_5$(*C*$_5$H$_{15}$)), 15.3 (CH$_2$*CH*$_3$), 25.3 (*CH*$_2$CH$_3$), 86.5 (aromatic), 86.9 (2CH, aromatic), 87.2 (2CH, aromatic), 95.3 (*C*$_5$(C$_5$H$_{15}$), 105.1 (*C*-CH$_2$CH$_3$), 121.5 (4CH, B(C$_6$H$_5$)$_4$), 125.3 (8CH, B(C$_6$H$_5$)$_4$), 135.5 (8CH, B(C$_6$H$_5$)$_4$), 162.3, 163.0, 163.7, 164.3 ppm (4CH, B(C$_6$H$_5$)$_4$, signals split by ^{11}B); ESMS (*m*/*z*): positive ion, calcd *m*/*z* for [(η^5-C$_5$(CH$_3$)$_5$)Ru(η^6-C$_6$H$_5$CH$_2$CH$_3$)$^+$]: 342.50, found: 343 (100%), negative ion, calcd *m*/*z* for B(C$_6$H$_5$)$_4^-$: 319.25, found: 319 (100%); elemental analysis, calcd (%) for C$_{42}$H$_{45}$BRu: C 76.2, H 6.87; found: C 76.1, H 6.82.

*[Ru(η^6-C$_6$H$_5$(CH$_2$)$_2$CH$_3$)(η^5-C$_5$(CH$_3$)$_5$)]BPh$_4$ (**4**)*

White powder, yield = 0.395 g, 74%; IR: $\tilde{\nu} = 3050$ (C–H aromatic, m, br), 2979 (C–H aliphatic, m, br), 2929 cm^{-1} (C–H aliphatic, w, br); NMR: ^{1}H ([D$_6$]DMSO): $\delta = 0.90$ (t, 3H, (CH$_2$)$_2$*CH*$_3$), 1.54 (m, 2H, CH$_2$*CH*$_2$CH$_3$), 1.89 (s, 15H, C$_5$(C$_5$H$_{15}$)), 2.25 (t, 2H, C*H*$_2$CH$_2$CH$_3$), 5.80–5.86 (m, 5H, C$_6$H$_5$), 6.76–6.80 (m, 4H, B(C$_6$H$_5$)$_4$ *para*), 6.90–6.93 (m, 8H, B(C$_6$H$_5$)$_4$ *meta*), 7.16–7.19 ppm (m, 8H, B(C$_6$H$_5$)$_4$ *ortho*); ^{13}C ([D$_6$]DMSO): $\delta = 10.0$ (C$_5$(*C*$_5$H$_{15}$)), 13.2 (CH$_2$)$_2$*C*H$_3$), 24.1 (*CH*$_2$CH$_2$CH$_3$), 33.8 (*CH*$_2$CH$_2$CH$_3$), 86.5 (aromatic), 87.2 (2CH, aromatic), 87.4 (2CH, aromatic), 95.3 (*C*$_5$-(C$_5$H$_{15}$), 103.5 (*C*– (CH$_2$)$_2$CH$_3$), 121.5 (4CH, B(C$_6$H$_5$)$_4$), 125.3 (8CH, B-(C$_6$H$_5$)$_4$), 135.5 (8CH, B(C$_6$H$_5$)$_4$), 162.3, 163.0, 163.7, 164.3 ppm (4CH, B-(C$_6$H$_5$)$_4$, signals split by ^{11}B); ESMS (*m*/*z*): positive ion, calcd *m*/*z* for [(η^5-C$_5$(CH$_3$)$_5$)Ru(η^6-C$_6$H$_5$(CH$_2$)$_2$CH$_3$)$^+$]: 356.53, found: 357 (100%), negative ion, calcd *m*/*z* for B(C$_6$H$_5$)$_4^-$: 319.25, found: 319 (100%); elemental analysis, calcd (%) for C$_{43}$H$_{47}$BRu: C 76.4, H 7.02; found: C 76.3, H 7.01.

*[Ru(η^6-C$_6$H$_5$CO$_2$CH$_2$CH$_3$)(η^5-C$_5$(CH$_3$)$_5$)]BPh$_4$ (**5**)*

White powder, yield = 0.277 g, 52%; IR: $\tilde{\nu} = 1727$ (C=O stretch, m), 1274 cm^{-1} (C–O stretch, m); NMR: ^{1}H ([D$_6$]DMSO): $\delta = 1.31$ (t, 3H, CH$_2$*CH*$_3$) 1.82 (s, 15H, C$_5$(C$_5$H$_{15}$)), 4.33 (q, 2H, C*H*$_2$CH$_3$), 6.07–6.09 (m, 3H, C$_6$H$_5$ *meta and para*), 6.34–6.38 (m, 2H, C$_6$H$_5$ *ortho*), 6.70–6.77 (m, 4H, B(C$_6$H$_5$)$_4$ *para*), 6.83–6.91 (m, 8H, B(C$_6$H$_5$)$_4$ *meta*), 7.11–7.13 ppm (m, 8H, B(C$_6$H$_5$)$_4$ *ortho*); ^{13}C ([D$_6$]DMSO): $\delta = 9.7$ (C$_5$(*C*$_5$H$_{15}$)), 14.1 (CH$_2$*CH*$_3$), 62.4 (*CH*$_2$CH$_3$), 86.5 (*C*–CO$_2$CH$_2$CH$_3$), 86.9 (2CH, aromatic), 88.3 (2CH, aromatic), 89.0 (aromatic), 97.1 (*C*$_5$(C$_5$H$_{15}$)), 121.5 (4CH, B-(C$_6$H$_5$)$_4$), 125.3 (8CH, B(C$_6$H$_5$)$_4$), 135.5 (8CH, B(C$_6$H$_5$)$_4$), 162.6, 163.1,

163.6, 164.1 ppm (4CH, $B(C_6H_5)_4$, signals split by ^{11}B), 164.3 (*C*=O); ESMS (*m/z*): positive ion, calcd *m/z* for $[(\eta^5\text{-}C_5(CH_3)_5)Ru(\eta^6\text{-}C_6H_5CO_2CH_2CH_3)^+]$: 386.51, found: 387 (100%), negative ion, calcd *m/z* for $B(C_6H_5)_4^-$: 319.25, found: 319 (100%); elemental analysis, calcd (%) for $C_{43}H_{45}O_2BRu$: C 73.2, H 6.40; found: C 73.4, H 6.47.

*[Ru(η⁶-C₆H₅CO₂CH₂CH₃)(η⁵-C₅(CH₃)₅)]BF₄ (**5a**)*

Bronze powder, yield = 0.235 g, 67%; IR: $\tilde{\nu}$ = 1727 (C=O stretch, s), 1295 cm^{-1} (C–O stretch, s); NMR: ^1H ([D₆]DMSO): δ = 1.31 (t, 3H, CH_2CH_3) 1.83 (s, 15H, $C_5(C_5H_{15})$), 4.34 (q, 2H, CH_2CH_3), 6.09–6.12 (m, 3H, C_6H_5 *meta and para*), 6.36–6.40 ppm (m, 2H, C_6H_5 *ortho*); ^{13}C ([D₆]DMSO): δ = 9.7 ($C_5(C_5H_{15})$), 14.1 (CH_2CH_3), 62.5 (CH_2CH_3), 86.5 (*C*-$CO_2CH_2CH_3$), 86.9 (2CH, aromatic), 88.3 (2CH, aromatic), 89.1 (aromatic), 97.1 ($C_5(C_5H_{15})$), 164.3 ppm (*C*=O); ESMS (*m/z*): positive ion, calcd *m/z* for $[(\eta^5\text{-}C_5(CH_3)_5)Ru(\eta^6\text{-}C_6H_5CO_2CH_2CH_3)^+]$: 386.51, found: 387 (100%), negative ion, calcd *m/z* for BF_4^-: 86.81, found: 87 (100%); elemental analysis, calcd (%) for $C_{19}H_{25}O_2BF_4Ru$: C 48.2, H 5.30; found: C 48.4, H 5.13.

*[Ru(η⁶-C₆H₅COCH₂CH₃)(η⁵-C₅(CH₃)₅)]BPh₄ (**7**)*

White powder, yield = 0.358 g, 70%; IR: $\tilde{\nu}$ = 1702 cm^{-1} (C=O stretch, s); NMR: ^1H ([D₆]DMSO): δ = 1.04 (t, 3H, CH_2CH_3) 1.80 (s, 15H, $C_5(C_5H_{15})$), 2.89 (q, 2H, CH_2CH_3), 6.08–6.10 (m, 3H, C_6H_5 *meta and para*), 6.43–6.45 (m, 2H, C_6H_5 *ortho*) 6.69–6.77 (m, 4H, $B(C_6H_5)_4$ *para*), 6.83–6.91 (m, 8H, $B(C_6H_5)_4$ *meta*), 7.09–7.16 ppm (m, 8H, $B(C_6H_5)_4$ *ortho*); ^{13}C ([D₆]DMSO): δ = 7.2 (CH_2CH_3) 9.8 ($C_5(C_5H_{15})$), 32.1 (CH_2CH_3), 85.8 (2CH, aromatic), 88.2 (2CH, aromatic), 89.1 (aromatic), 91.4 (*C*-$COCH_2CH_3$), 96.9 ($C_5(C_5H_{15})$), 121.5 (4CH, $B(C_6H_5)_4$), 125.3 (8CH, B-$(C_6H_5)_4$), 135.5 (8CH, $B(C_6H_5)_4$), 162.6, 163.1, 163.6, 164.1 ppm (4CH, B-$(C_6H_5)_4$, signals split by ^{11}B), 199.3 (*C*=O); ESMS (*m/z*): positive ion, calcd *m/z* for $[(\eta^5\text{-}C_5(CH_3)_5)Ru(\eta^6\text{-}C_6H_5COCH_2CH_3)^+]$: 370.51, found: 371 (100%), negative ion, calcd *m/z* for $B(C_6H_5)_4^-$: 319.25, found: 319 (100%); elemental analysis, calcd (%) for $C_{43}H_{45}OBRu$: C 74.9, H 6.59; found: C 74.54, H 6.41.

*[Ru(η⁶-C₁₀H₈)(η⁵-C₅(CH₃)₅)]BPh₄ (**10**)*

Yellow crystals, yield = 0.403 g, 75%; IR: $\tilde{\nu}$ = 3050 (C–H aromatic, m, br), 2975 (C–H aliphatic, m, br), 2928 cm^{-1} (C–H aliphatic, w, br); NMR: ^1H ([D₆]DMSO): δ = 1.59 (s, 15H, $C_5(C_5H_{15})$), 6.11–6.13 (m, 2H, aromatic (B & C)), 6.67–6.69 (m, 2H, aromatic (A & D)), 6.75–6.80 (m, 4H, B-$(C_6H_5)_4$ *para*), 6.89–6.94 (m, 8H, $B(C_6H_5)_4$ *meta*), 7.14–7.20 (m, 8H, B-$(C_6H_5)_4$ *ortho*), 7.60–7.64 (m, 2H, aromatic (E & G)), 7.66–7.70 ppm (m, 2H, aromatic (E & H)); ESMS (*m/z*): positive ion, calcd *m/z* for $[(\eta^5\text{-}C_5(CH_3)_5)Ru(\eta^6\text{-}C_{10}H_8)^+]$: 364.50, found: 365 (100%), negative ion, calcd *m/z* for $B(C_6H_5)_4^-$: 319.25, found: 319 (100%); elemental analysis, calcd (%) for $C_{44}H_{43}BRu$: C 77.3, H 6.35; found: C 77.1, H 6.38.

*[Ru(η⁶-C₁₄H₁₀)(η⁵-C₅(CH₃)₅)]BPh₄ (**11**)*

Cream crystals, yield = 0.414 g, 64%; IR: $\tilde{\nu}$ = 3053 (C–H aromatic, m, br), 2983 (C–H aliphatic, w, br), 2930 cm^{-1} (C–H aliphatic, w, br); NMR: ^1H ([D₆]DMSO): δ = 1.45 (s, 15H, $C_5(C_5H_{15})$), 6.19–6.24 (m, 2H, aromatic (B & C)), 6.62–6.64 (m, 1H, aromatic (D)), 6.76–6.80 (m, 4H, $B(C_6H_5)_4$ *para*), 6.89–6.93 (m, 8H, $B(C_6H_5)_4$ *meta*), 7.12–7.17 (m, 8H, $B(C_6H_5)_4$ *ortho*), 7.39–7.42 (m, 2H, aromatic (H & I)), 7.78–7.80 (m, 2H, aromatic (A & E)), 7.98–8.03 (m, 2H, aromatic (F & G)), 8.57–8.59 ppm (m, 1H, aromatic (J)); ESMS (*m/z*): positive ion, calcd *m/z* for $[(\eta^5\text{-}C_5(CH_3)_5)Ru(\eta^6\text{-}C_{14}H_{10})^+]$: 414.56, found: 415 (100%), negative ion, calcd *m/z* for $B(C_6H_5)_4^-$: 319.25, found: 319 (100%); elemental analysis, calcd (%) for $C_{48}H_{45}BRu$: C 78.6, H 6.19; found: C 78.6, H 6.10.

*[Ru(η⁶-C₁₆H₁₀)(η⁵-C₅(CH₃)₅)]BPh₄ (**12**)*

Yellow crystals, yield = 0.182 g, 31%; IR: $\tilde{\nu}$ = 3051 (C–H aromatic, m, br), 2980 (C–H aliphatic, w, br), 2934 cm^{-1} (C–H aliphatic, w, br); NMR: ^1H ([D₆]DMSO): δ = 1.26 (s, 15H, $C_5(C_5H_{15})$), 6.36–6.39 (m, 1H, aromatic (B)), 6.75–6.77 (m, 2H, aromatic (A & C)), 6.75–6.79 (m, 4H, $B(C_6H_5)_4$ *para*), 6.89–6.93 (m, 8H, $B(C_6H_5)_4$ *meta*), 7.13–7.19 (m, 8H, $B(C_6H_5)_4$ *ortho*), 7.72–7.74 (m, 2H, aromatic (D & J)), 8.08–8.12 (m, 1H, aromatic (7)), 8.26–8.29 ppm (m, 4H, aromatic (E, F, H & J)); ESMS (*m/z*): positive ion, calcd *m/z* for $[(\eta^5\text{-}C_5(CH_3)_5)Ru(\eta^6\text{-}C_{16}H_{10})^+]$: 438.58, found: 439 (100%), negative ion, calcd *m/z* for $B(C_6H_5)_4^-$: 319.25, found: 319 (100%); elemental analysis, calcd (%) for $C_{50}H_{45}BRu$: C 79.3, H 6.00; found: C 79.1, H 5.95.

Crystallography

Unique data sets were collected on an Oxford Diffraction GEMINI S Ultra CCD diffractometer (compounds **4**, **5a**, **10,** and **12**) and a Rigaku AFC 7R four-circle diffractometer (compound **11**) utilizing Mo K_α radiation. The structures were solved by direct methods and refined by full-matrix least-squares refinement on F^2 after application of semiempirical absorption corrections. Anisotropic thermal parameters were refined for non-hydrogen atoms; (x, y, z, $U_{iso})_H$ were included and constrained at estimated values. Conventional residuals at convergence are quoted; statistical weights were employed. Computation was done using the CrysAlis, teXsan, SHELX97, and ORTEP-3 program and software systems.[21] CCDC 821740, CCDC 821741, CCDC 821742, CCDC 821743, and CCDC 821744 contain the supplementary crystallographic data for this paper. These data can be obtained free of charge from the Cambridge Crystallographic Data Centre via www.ccdc.cam.ac.uk/data_request/cif.

Computational Calculations

The Gaussian 03 computer package[22] was employed for all calculations incorporating the Hartree–Fock theory in the case of the geometry optimizations and the second-order Møller–Plesset perturbation theory (MP2) for single point calculations.[17] Geometry optimization calculations for complexes **3**, **6**, **7**, and **9** were performed in the gas phase using the LanL2DZ basis set.[18] Electrostatic potential surfaces for complexes **1**–**12** were calculated from the density matrices generated by single point calculations at the MP2 level using the cc-pVDZ basis set[19] for all atoms, with Ru parameters adjusted for the inclusion of a pseudo potential. The magnitude of the electrostatic potential is represented using a color scale ranging from red (0.00 au) to blue (+0.12 au).

Cell Culture and Cytotoxic Evaluation

Each cell line was cultured at 37 °C in RPMI 1640 medium supplemented with heat-inactivated fetal calf serum (10%, CSL, Australia), 3 mM HEPES buffer (pH 7.3–7.4), penicillin (100 U mL^{-1}), and streptomycin (100 μg mL^{-1}) at 5% CO_2 and 99% humidity. Primary human fibroblasts were obtained from neonatal foreskin cultured in the above medium. Culture media were replaced every three days, and cell monolayers were split at 70–80% confluency. Routine mycoplasma tests were performed using Hoechst stains and were always negative.

Stock solutions of each complex were prepared by dissolving the compounds (ca. 10 mg) in ethanol (1 mL). These stock solutions were diluted as necessary for testing. Cells were seeded in 96-well microtiter plates at approximately 5000 cells per 100 μL (NFF), 3000 cells per 100 μL (MCF7, MDA-MB-231, CI80-13S, T47-D, DU145, PC3, HT29, A549, MM418c5, B16, RAW264), and 1000 cells per 100 μL (MM96L). Seven dilutions of each drug were added to triplicate wells. The plates were incubated for 6 days prior to incorporation of the SRB staining method.[20] The culture medium was removed from the plates and each plate washed with phosphate-buffered saline (PBS). The plates were fixed with methylated spirit for 15 min and then washed with water. SRB solution (50 μL, 0.4% SRB dye (w/v) in 1% (v/v) acetic acid) was added to each well and left at room temperature for 45 min. The SRB solution was removed and the plates washed quickly, once with water and twice with 1% (v/v) acetic acid solution. For the NFF cell assay, the plates were washed thrice with 1% (v/v) acetic acid solution. Tris base (100 μL, 10 mM, unbuffered, pH > 9) was added to each well to solubilize the protein-bound dye. After incubation for 5 min, the absorbance was measured at 564 nm on a multiwell plate reader. The percentage of surviving cells was calculated from the absorbance of untreated control cells. The IC_{50} values for the inhibition of cell viability were determined by fitting the plots of the percentage of surviving cells against drug concentration using a sigmoidal function.

CHEMISTRY
AN ASIAN JOURNAL

Acknowledgements

We thank the Eskitis Institute for Cell and Molecular Therapies, the Queensland Micro- and Nanotechnology Facility, and the Queensland Institute of Medical Research for their support of this project.

[1] a) T. W. Hambley, *Science* **2007**, *318*, 1392; b) M. E. Bravo-Gomez, L. Ruiz-Azuara in *New Approaches in the Treatment of Cancer*, Nova Science Publishers, Inc., Hauppauge, **2010**, pp. 139; c) H. R. Hansen, O. Farver in *Textbook of Drug Design and Discovery*, Edition. 4, University of Copenhagen, **2010**, pp. 151.

[2] a) E. Wong, C. M. Giandomenico, *Chem. Rev.* **1999**, *99*, 2451; b) D. Wang, S. J. Lippard, *Nat. Rev. Drug Discovery* **2005**, *4*, 307.

[3] S. H. van Rijt, P. J. Sadler, *Drug Discovery Today* **2009**, *14*, 1089.

[4] a) S. P. Fricker, *Dalton Trans.* **2007**, 4903; b) J. M. Rademaker-Lakhai, D. Van Den Bongard, D. Pluim, J. H. Beijnen, J. H. M. Schellens, *Clin. Cancer Res.* **2004**, *10*, 3717; c) C. G. Hartinger, M. A. Jakupec, S. Zorbas-Seifried, M. Groessl, A. Egger, W. Berger, H. Zorbas, P. J. Dyson, B. K. Keppler, *Chem. Biodiversity* **2008**, *5*, 2140; d) F. Lentz, A. Drescher, A. Lindauer, M. Henke, R. A Hilger, C. G. Hartinger, M. E. Scheulen, C. Dittrich, B. K. Keppler, U. Jaehde, *Anti-Cancer Drugs* **2009**, *20*, 97.

[5] C. G. Hartinger, P. J. Dyson, *Chem. Soc. Rev.* **2009**, *38*, 391.

[6] a) J. E. Clark, P. Naughton, S. Shurey, C. J. Green, T. R. Johnson, B. E. Mann, R. Foresti, R. Motterlini, *Circ. Res.* **2003**, *93*, 178; b) W. Beck, K. Severin, *Chem. Unserer Zeit* **2002**, *36*, 356; c) A. Kascatan-Nebioglu, M. J. Panzner, C. A. Tessier, C. L. Cannon, W. J. Youngs, *Coord. Chem. Rev.* **2007**, *251*, 884; d) D. Colangelo, A. Ghiglia, A. Ghezzi, M. Ravera, E. Rosenberg, F. Spada, D. Osella, *J. Inorg. Biochem.* **2005**, *99*, 505; e) Y. K. Yan, M. Melchart, A. Habtermariam, P. J. Sadler, *Chem. Commun.* **2005**, 4764.

[7] a) A. F. A. Peacock, P. J. Sadler, *Chem. Asian J.* **2008**, *3*, 1890; b) W. H. Ang, A. Casini, G. Sava, P. J. Dyson, *J. Organomet. Chem.* **2011**, *696*, 989.

[8] a) M. H. Garcia, A. Valente, P. Florindo, T. S. Morais, M. F. M. Piedade, M. T. Duarte, V. Moreno, F. X. Aviles, J. Loreno, *Inorg. Chim. Acta* **2010**, *363*, 3765; b) B. T. Loughrey, P. C. Healy, P. G. Parsons, M. L. Williams, *Inorg. Chem.* **2008**, *47*, 8589.

[9] a) B. T. Loughrey, M. L. Williams, P. C. Healy, A. Innocenti, D. Vullo, C. T. Supuran, P. G. Parsons, S-A. Poulsen, *J. Biol. Inorg. Chem.* **2009**, *14*, 935; b) B. T. Loughrey, M. L. Williams, T. J. Carruthers, P. G. Parsons, P. C. Healy, *Aust. J. Chem.* **2010**, *63*, 245; c) L. S. Micallef, B. T. Loughrey, P. C. Healy, P. G. Parsons, M. L. Williams, *Organometallics* **2010**, *29*, 6237; d) L. S. Micallef, B. T. Loughrey, P. C. Healy, P. G. Parsons, M. L. Williams, *Organometallics* **2011**, *30*, 1395.

[10] a) S. J. Berners-Price, A. Filipovska, *Aust. J. Chem.* **2008**, *61*, 661; b) D. Pathania, M. Millard, N. Neamati, *Adv. Drug Delivery Rev.* **2009**, *61*, 1250; c) S. Fulda, L. Galluzzi, G. Kroemer, *Nat. Rev. Drug Discovery* **2010**, *9*, 447.

[11] a) J. L. Schrenk, A. M. McNair, F. B. McCormick, K. R. Mann, *Inorg. Chem.* **1986**, *25*, 3501; b) T. D. Tilley, R. H. Grubbs, J. E. Bercaw, *Organometallics* **1984**, *3*, 274.

[12] a) P. J. Fagan, M. D. Ward, J. C. Calabrese, *J. Am. Chem. Soc.* **1989**, *111*, 1698; b) R. M. Fairchild, K. T. Holman, *Organometallics* **2007**, *26*, 3049; c) U. Kölle, J. Kossakowski, R. Boese, *J. Organomet. Chem.* **1989**, *378*, 449; d) U. Koelle, M. H. Wang, *Organometallics* **1990**, *9*, 195; e) W. S. Sheldrick, A. J. Gleichmann, *J. Organomet. Chem.* **1994**, *470*, 183.

[13] A. R. Kudinov, M. I. Rybinskaya, Y. T. Struchkov, A. I. Yanovskii, P. V. Petrovskii, *J. Organomet. Chem.* **1987**, *336*, 187.

[14] a) C. Gemel, K. Mereiter, R. Schmid, K. Kirchner, *Organometallics* **1996**, *15*, 532; b) M. E. Navarro Clemente, P. Juarez Saavedra, M. Cervantes Vasquez, M. A. Paz-Sandoval, A. M. Arif, R. D. Ernst, *Organometallics* **2002**, *21*, 592.

[15] a) E. Clar in *The Aromatic Sextet*, Wiley, London, **1972**; b) K. P. Vijayalakshmi, C. H. Suresh, *New J. Chem.* **2010**, *34*, 2132.

[16] a) U. Koelle, M. H. Wang, G. Raabe, *Organometallics* **1991**, *10*, 2573; b) D. Morvan, T. B. Rauchfuss, S. R. Wilson, *Organometallics* **2009**, *28*, 3161.

[17] C. Møller, M. S. Plesset, *Phys. Rev.* **1934**, *46*, 618.

[18] P. J. Hay, W. R. Wadt, *J. Chem. Phys.* **1985**, *82*, 270.

[19] a) T. H. Dunning, *J. Chem. Phys.* **1989**, *90*, 1007; b) K. A. Peterson, D. Figgen, M. Dolg, H. Stoll, *J. Chem. Phys.* **2007**, *126*, 124101.

[20] P. Skehan, R. Storeng, D. Scudiero, A. Monks, J. McMahon, D. Vistica, J. T. Warren, H. Bokesch, S. Kenney, M. R. Boyd, *J. Natl. Cancer Inst.* **1990**, *82*, 1107.

[21] a) Oxford Diffraction, *CrysAlis PRO*. Oxford Diffraction Ltd, Yarnton, England, **2010**; b) Molecular Structure Corporation, *TeXsan for Windows*, Version 1.06, MSC 9009 New Trails Drive, The Woodlands, TX 77381, USA, **1997**–**2001**; c) G. M. Sheldrick, *Acta Crystallogr. Sect. E* **2008**, *A64*, 112; d) L. J. Farrugia, *J. Appl. Crystallogr.* **1997**, *30*, 565.

[22] *Gaussian 03*, Revision D.01, M. J. Frisch, G. W. Trucks, H. B. Schlegel, Gaussian Inc., Wallingford CT, USA, **2004**.

Received: July 22, 2011
Published online: November 17, 2011

